Experimental specific heat of iron, cobalt, and nickel clusters studied in a molecular beam

Daniele Gerion,* Armand Hirt, I. M. L. Billas,† A. Châtelain, and W. A. de Heer‡
Institut de Physique Expérimentale, Département de Physique, Ecole Polytechnique Fédérale de Lausanne, CH-1015 Lausanne, Switzerland

(Received 3 May 1999; revised manuscript received 15 May 2000)

Specific heat measurements on free iron, cobalt and nickel clusters in different size ranges from 130 to 400 atoms are presented and the experimental method is discussed in detail. These measurements are achieved in a Stern-Gerlach experiment where the magnetization of transition metal clusters reflects their vibrational temperature. Hence, it can be used as a thermometer after a calibration procedure. The specific heat is measured by heating the clusters in flight with a laser. In the temperature range of the experiment (80–600 K), the main feature of the specific heat of $Ni_{200-240}$ clusters is a broad peak centered at $T=340$ K which adds to an approximately constant baseline of 6 cal/(mol K). We attribute this peak to a ferro- to paramagnetic transition since its shape and area are well described by the Weiss mean field model. The specific heat of $Co_{200-240}$ clusters does not show any prominent feature within the temperature range 80–900 K except a steady increase from 5.5 cal/(mol K) at $T=300$ K to 15 cal/(mol K) at $T=900$ K. In iron clusters, the specific heat exhibits a peak which is poorly described by a Weiss mean field theory. Furthermore, the specific heat value of $Fe_{250-290}$ clusters at room temperature is up to 50% lower than the Dulong-Petit value. We discuss the possibility that iron clusters undergo a magnetic transition between a high moment to a low moment state, which have different lattice parameters.

I. INTRODUCTION

The modifications to the properties associated with phase transitions due to finite size effects have promoted for many decades extensive theoretical and experimental investigations. [1–18] A large fraction of the theoretical[1–8] as well as of the experimental[12–18] work performed in this area has been devoted to the study of the solid-to-solid[11] and solid-to-liquid[2–5,12–14] phase transitions in finite size systems. Investigations of second order phase transitions in cluster systems, like the ferromagnetic-to-paramagnetic phase transition,[6,7,15–17] are scarce and almost exclusively limited to theoretical studies. In this case, Monte Carlo simulations of finite Heisenberg clusters[6] predict a rounding of the ferromagnetic to paramagnetic transition as well as a lowering of the transition temperature. These effects are due to the reduced coordination of the spins at the cluster surface favoring larger spin fluctuations. In fact, the lowering of the transition temperature is already predicted in the simple mean field picture[19,20] where the critical temperature is directly proportional to the coordination number. In addition, the spins at the cluster surface have larger amplitudes due to their lower coordination. In the Heisenberg model, large spins tend to increase the transition temperature while the reduction of the coordination acts to decrease it. Thus, Heisenberg clusters, with different surface to volume ratios, might exhibit a thermal evolution that depends on a delicate balance between these competing effects.

This complexity is reflected in the magnetic properties of $3d$ transition metal clusters.[15–17] While in nickel and cobalt clusters with increasing size, the magnetic moments per atom as a function of temperature are found to converge to the respective bulk values, in iron clusters the magnetic moment curves depart seriously from the bulk curve for all investigated sizes. In iron clusters, the magnetic moment decreases markedly from its low temperature value well below the bulk iron Curie temperature (1043 K). Furthermore, iron clusters in different size ranges exhibit a radically different thermal behavior. For instance, iron clusters with 120 to 140 atoms have a qualitatively different thermal evolution compared to iron clusters with 250 to 290 atoms. In the former case, the magnetic moment is approximately constant at 3 μ_B below 350 K and drops to about 0.7 μ_B at 700 K, to augment again slightly at higher temperatures. In the latter case, the magnetic moment decreases continuously and smoothly with increasing temperature up to 700 K, where it levels off at about 0.4 μ_B. This value is much larger than the one predicted by calculations of Heisenberg cluster spin systems at temperatures above the transition temperature[6,16] and more generally the shape of the calculated magnetic moment curve also differs radically from the experimental one. The nature of Fe cluster transitions is a delicate issue. Guided by the complex thermal dependence of the iron bulk specific heat, it was suggested that a structural change drives the magnetic disorder.[16]

In the bulk, the specific heat is a powerful tool to investigate phase transitions, since it exhibits large variations near critical points. The energy involved in the second order transitions is experimentally obtained as the peak surface in the specific heat curve. For instance, in bulk iron,[21] the energy associated with the magnetic transition at 1043 K (1930 cal/mol) is about 40% lower than the latent heat of fusion (3303 cal/mol) which occurs at 1811 K. Beside the magnetic and the melting transitions, bulk iron shows crystallographic phase transitions, at 1185 K from bcc to fcc and at 1667 K from fcc back to bcc. However, the energies associated with these phase transitions are smaller than the magnetic energy: 215 cal/mol for the former one and 202 cal/mol for the latter one. Although iron differs from nickel and cobalt in its polymorphic character, these two latter metals with a considerably simpler phase diagram show about the same ratio of energy between magnetic and melting transitions as iron. In

the light of the above considerations, specific heat measurements of small ferromagnetic clusters could give a deeper insight on the mechanism responsible for the magnetic transition.

For free clusters, we define the specific heat as the ratio between the variation of the total energy of the cluster and the variation of its temperature, i.e., $C = \Delta E/\Delta T$ (without mention of the thermodynamic process through which the total energy is changed). Stern-Gerlach (S-G) measurements on ferromagnetic iron, cobalt and nickel clusters[18] indicate that the cluster lattice vibrations act as a thermal bath for the spin system: this allows clusters to have an internal thermometer, namely their magnetization. The specific heat measurement method is based on the following idea. The clusters are illuminated with a laser light and modifications to their magnetic properties compared to the non-illuminated case are recorded in a Stern-Gerlach experiment. When illuminated with a laser of characteristic frequency ω, the cluster absorbs a given number n of photons, each with an energy $\hbar\omega$, and hence its total energy is increased by $n\hbar\omega$. The impinging photons are absorbed by the electronic cloud. This energy excess is quickly relaxed, in a radiationless process, into the vibrations causing a variation of the temperature. Since the magnetization of ferromagnetic clusters depends on their vibrational temperature, the temperature increase due to photon absorption provokes a variation in their magnetization, which is probed by measuring the change in the S-G deflections.

This report is organized as follows: in Sec. II we describe the experimental setup and the basic measurement principles. Section III gives a deeper insight of the specific heat measurements; we explain our method and justify our assumptions. Finally in Sec. IV, we present and discuss the results on nickel, cobalt, and iron clusters.

II. EXPERIMENTAL SETUP

The experimental setup has been described extensively elsewhere.[16,22] A frequency doubled pulsed Nd:YAG laser (532 nm, 10 Hz, 100 mJ/pulse, pulse duration of 10 ns) fires onto a pure material rod. The formed plasma condenses into clusters in a helium buffer gas. The mixture spends about 1–2 ms in a nozzle whose temperature can be varied from 78 K to 1000 K. This time is long enough to ensure a thermalization: the cluster vibrational temperature is very close to the nozzle temperature (see Ref. 16 and references therein). The expansion into vacuum does not affect the cluster vibrational temperature when adequate source operating conditions are selected. This affirmation is based on previous studies where magnetic properties have been thoroughly investigated for these operating conditions. A chopper wheel allows velocity measurements and defines the whole timing of the experiment. The cluster beam is collimated and then passes through an inhomogeneous magnetic field where clusters are deflected. The beam deflection d depends on the applied magnetic field H, the cluster velocity v and the cluster magnetization $M(T)$ according to the following formula:

$$d = \chi \frac{M(T)H}{v^2}, \tag{1}$$

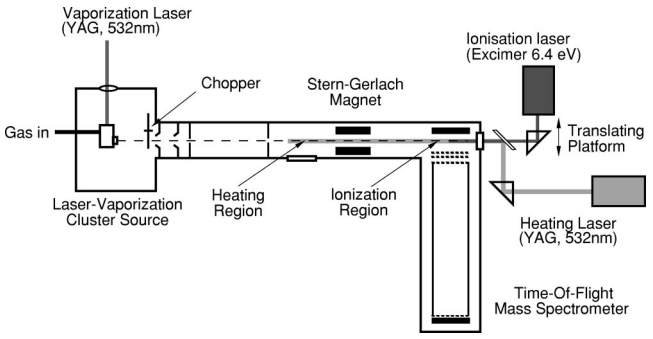

FIG. 1. Overview of the experimental apparatus. The heating laser enters collinearly with the cluster beam and interacts with it before the beam enters the Stern-Gerlach magnet.

where χ is a constant which depends on the geometry of the experiment. The magnetization represents the time average projection of the cluster magnetic moment onto the field direction, i.e., $M(T) = |\boldsymbol{\mu}(T) \cdot \boldsymbol{H}|/H$. $\mu(T)$ is the temperature dependent magnetic moment of the cluster, a quantity analogous to the magnetic moment of bulk materials which is deduced from the magnetization at saturation.[15–17]

One meter downstream from the magnet, a narrow collinear excimer laser light beam (1 mm wide, ArF 6.4 eV) ionizes the clusters which are then accelerated perpendicularly in a time-of-flight mass spectrometer (TOFMS). The drift time of the clusters in the TOFMS is independent of the position where the clusters have been ionized, but depends on the cluster mass, and thus permits a size selection.[22] The slit of the ionizing laser light is swept across the ionization region. The intensity corresponding to a selected cluster size range is measured for each slit position so that the beam profile can be mapped out. Performing this type of measurement with and without applied magnetic field allows the cluster beam deflections to be measured. The deflections correspond to the profile center of mass, which is extracted by a very accurate method. It involves the convolution of a broad Gaussian and the data. The maximum's position of this convoluted spectrum is then determined. This method has been extensively tested in simulations and experiments and has been found to be more reliable than the simple procedure that determines the first moment of the deflection profile. Then, from the knowledge of the cluster velocity, the cluster magnetization in a given size range can be determined as a function of temperature with Eq. (1).

In specific heat measurements, the cluster beam is illuminated collinearly by a frequency doubled Nd:YAG laser (532 nm, a few mJ/pulse, pulse duration of 10 ns) about 15 cm before it enters the Stern-Gerlach magnet (Fig. 1). We make sure that the region where the cluster beam is heated is uniformly illuminated by looking at the laser light shadow through the magnet poles. The laser intensity is measured at the entrance of the vacuum chamber, and is directly proportional to the fluence of the laser light in the interaction region. In the experiment, a magnetic field is applied and the cluster velocity is measured. Then, the heated and the non-heated cluster beam profiles are recorded in a single scan by measuring alternatively their corresponding cluster beam intensity for each position of the ionizing light slit. Beam profiles are mapped out at fixed magnetic field strength for different heating laser light intensities. In this manner, we make

sure that fragmentation is negligible since both heated and nonheated cluster profiles are seen to have the same intensity. The cluster specific heat is then determined from the deflections of the beam profiles with respect to the undeflected beam as explained in the next section.

III. SPECIFIC HEAT MEASUREMENTS

A. Generalities

The specific heat measurement relies on the consideration that the free cluster total energy can be modified by two different processes: first, by increasing its internal energy through photon absorption; secondly, by increasing its temperature through thermalization in the source with a heated buffer gas. Both processes lead to a thermal disorder of the atomic magnetic moments inside the cluster and hence to a reduction of the cluster magnetic moment and magnetization. The reduction in magnetization is experimentally revealed by smaller cluster beam deflections compared to a similar but nonheated experiment [see Eq. (1)].

The photoabsorption and thermalization processes lead to equivalent internal energy and temperature increases. Indeed, the photon absorption occurs through the electronic cloud. The relaxation of the absorbed energy into vibrational and electronic degrees of freedom takes place on a very short time scale of about 10–100 ps.[23] The energy relaxation is completed well before the cluster enters the Stern-Gerlach magnet. Therefore, both heating processes affect the cluster magnetization similarly. In other words, the cluster magnetization acts as a sensitive thermometer for free clusters.

The measurement of the cluster magnetization $M(T)$ has been performed under experimental conditions where $M(T)$ follows a superparamagnetic behavior,[24] i.e., $M(T) \propto \mu^2(T)/T$. However, the experimental and analysis methods used to obtain the cluster specific heat do not depend on the superparamagnetic assumption and are generally applicable.

Consider the interaction of a cluster beam at temperature T with a laser light of intensity I. During the short laser pulse, clusters absorb a certain number n of photons with a probability distribution $P(n,\beta I)$ given by the Poisson statistics, $P(n,\beta I)=e^{-\beta I}(\beta I)^n/n!$. Here β is the photoabsorption cross section, which is assumed to be temperature independent. βI represents the mean number of absorbed photons and can be experimentally determined as explained in Sec. III C.

We use relatively low heating light intensities so that the clusters absorb a limited number of photons, maximally 5–10. Since the heating process lasts several nanoseconds and each absorption relaxes on a picosecond time scale, each absorption event can be considered independent of the other ones. The first absorbed photon increases the cluster temperature from T to $T+\Delta T_1$, where $\Delta T_1=\hbar\omega/C(T)$ is the product of the photon energy times the inverse of the cluster specific heat at temperature T. The second absorbed photon increases the temperature from $T+\Delta T_1$ up to $T+\Delta T_1+\Delta T_2$. This absorption process involves the specific heat at temperature $T+\Delta T_1$. In the general case where n photons are absorbed, the task of determining the corresponding temperature increase from the measurements gets quickly very complicated. We simplify the problem by assuming that each photon produces the same temperature increase $\Delta T_n=\Delta T$.[25] This assumption is justified by the fact that the laser intensities used in the experiment were relatively low and the clusters studied quite large, such that the temperature increase due to the absorption of one photon is modest (a few to a few tens of degrees).

The effect of the temperature increase on the magnetization is thus described by

$$\langle M\rangle=\sum_{n\geqslant 0} M(T+n\Delta T)P(n,\beta I), \tag{2}$$

where $\langle M\rangle$ is the mean magnetization of the heated cluster beam and $P(n,\beta I)$ is the Poisson probability distribution defined above. The numerical evaluation of $\langle M\rangle$ with Eq. (2) involves limiting n to an arbitrary maximal number of absorbed photons. Ignoring the high n terms in the expression has a negligible effect on the final result, because of the n-factorial decreasing terms in the sum.

Ideally, it should be possible to observe the effects of the discrete photon absorption on the magnetization. Namely, the whole deflection profile should be composed of discrete peaks, each one corresponding to the deflection profile of clusters which have absorbed the same number of photons. The spikes corresponding to both zero and one photon absorption should indicate how the magnetization, and hence the temperature, changes after an internal energy increase of $\hbar\omega$. This procedure does not require the explicit knowledge of the photoabsorption cross section in order to determine the specific heat. Unfortunately, multispike structures in the cluster profiles cannot be observed because the high collimation of the cluster beam required for their observation is not attained experimentally, and because the deflection process in the SG magnet naturally involves some broadening of the cluster beam. In fact we observe that higher heating laser intensities lead to lower deflections because of the larger mean number of absorbed photons (Fig. 2).

Note that the heated profiles present a deformed shape that renders difficult an analysis based directly on the profile shapes. Indeed, the deconvolution of the heated profiles into basis profiles, corresponding to clusters having absorbed a different number of photons, was found to be sensitive to small irregularities in the profile shapes. Moreover, an accurate deconvolution required at least several tens of basis profiles. The method detailed in Sec. III B overcomes these technical limitations. It allows the contribution of the one-photon absorption process to the total deflection peak to be extracted and hence permits a direct measurement of the specific heat. Besides, a second method, experimentally and conceptually simpler than the first one, is used to measure the specific heat relative to an existing calibration measurement. It is described in Sec. III C.

B. Absolute determination of the cluster specific heat

In the limit of low laser intensities the events involving more than one photon become negligible: the probability to absorb 2 or more photons becomes very small compared to the 0 and 1 photon absorption probabilities as indicated by Eq. (2). Further in this section, we will explain how this situation can be actually achieved experimentally. For now, let us assume that the heating light intensity is so low that clusters absorb only zero or one photon. In this case, the

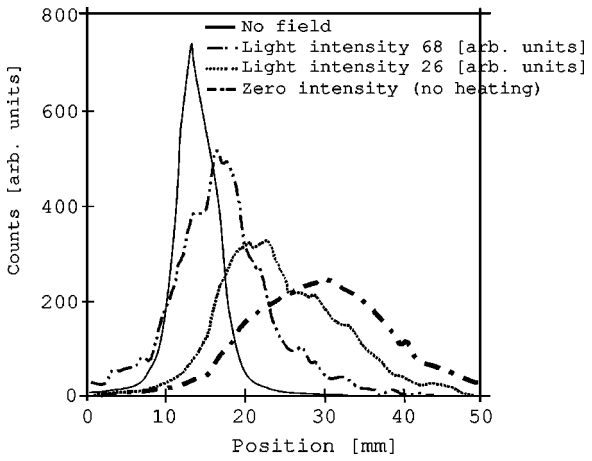

FIG. 2. Typical cluster beam deflection profiles. The continuous profile corresponds to clusters which are not deflected. Its amplitude has been divided by 1.33 for figure convenience. By applying a magnetic field we observe a deflection of the beam profile, noted ''zero intensity'' on the graph. By illuminating the beam and keeping the magnetic field constant, we measure less deflected profiles. The deflection corresponds to the profile center of mass. A higher laser light intensity leads to a smaller deflection. We do not observe a multispike structure but a single peak profile.

heated cluster beam deflection profile $\psi(r,H)$ is composed of the deflection profiles $\psi_0(r,H)$ and $\psi_1(r,H)$ corresponding to clusters which have absorbed zero photon (and have a temperature T) and one photon (with corresponding temperature $T+\Delta T$) respectively. Hence,

$$\psi(r,H)=(1-\alpha)\psi_0(r,H)+\alpha\psi_1(r,H), \tag{3}$$

where α is the probability for absorbing one photon. At the intersection point of the profiles $\psi(r,H)$ and $\psi_0(r,H)$ [i.e., at the position r^* where $\psi(r^*,H)=\psi_0(r^*,H)$], we find from Eq. (3) that $\alpha[\psi_0(r^*,H)-\psi_1(r^*,H)]=0$. This intersection point r^* is therefore independent of α and hence of the laser intensity I.

In our experiment, the profiles $\psi(r,H)$ and $\psi_0(r,H)$ are recorded simultaneously in a single scan. The analysis method then used to extract $\psi_1(r,H)$ from the measured profile $\psi(r,H)$ uses the dependence of the deflection d on the product $H\,M(T)$, where H is the deflecting magnetic field and $M(T)$ is the cluster magnetization. $M(T)$ is a monotonous decreasing function known from previous investigations of magnetic clusters.[15,16] From the relation $d \propto H\,M(T)$, it follows that the profile $\psi_1(r,H)$, corresponding to the one-photon heated clusters (whose temperature is $T+\Delta T$) and deflected by a magnetic field H, is equivalent to a profile $\psi'(r,H')$ corresponding to nonheated clusters (whose temperature is T) deflected by a lower magnetic field $H'<H$.[26] In order to determine H', we measure a set of profiles using several different deflecting fields $\{\psi_0(r,H_1),\psi_0(r,H_2),\ldots,\psi_0(r,H_N)\}$. The set of reference profiles is obtained at temperature T, in the absence of laser heating. We then deduce, by interpolation in the set, the profile $\psi_0(r,H')$ which intersects the profile $\psi_0(r,H)$ at the point r^*.

If the clusters were restricted to absorb no more than one photon, then the value of H' obtained by the preceding procedure would be the same for each laser intensity because it is independent of α. Nevertheless if several photons can also be absorbed, it can be shown that H' becomes a function of the laser intensity with the same value in the zero intensity limit. By developing Eq. (3) at higher orders, it can be deduced that the dependence in intensity is linear if up to two photons are absorbed, quadratic if up to three photons are absorbed and so on. For the laser intensities that we used in this calibration procedure, our results display a linear dependence (Fig. 3). This indicates that we have reached the experimental condition where less than two photons are absorbed. Indeed, as we will point out in Sec. III C, the probability to absorb three or more photons is lower than 0.6% for the intensity range of Fig. 3.

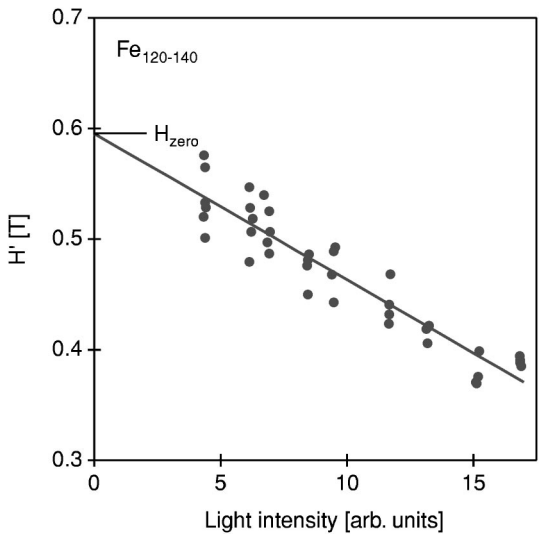

FIG. 3. The extrapolated field for the calibration of the specific heat of $Fe_{120-140}$ clusters at room temperature. The continuous line is a linear fit to the experimental results. Strictly speaking they correspond to the deflecting magnetic field which simulates the temperature increase caused by the absorption of a single photon as a function of the heating laser light intensity. What we call the extrapolated field H_{zero} is the value of the linear fit in the limit of zero intensity. Our model indicates that the dependence of the extrapolated field on the intensity should be linear if less than three photons are absorbed. In the case of $Fe_{120-140}$ atoms, the best field is 0.59 T, which corresponds to $\Delta T=100.7$ K hence a specific heat $C=4.02$ cal/(mol K).

The extrapolated magnetic field corresponding to the zero intensity case is

$$H_{\mathrm{zero}}=\lim_{I\to 0} H'. \tag{4}$$

It gives the value of an hypothetical field that, applied on the cluster beam, would deflect it by the same amount as the actual field H deflects the particles having absorbed one photon. It allows the determination of the temperature increase corresponding to a one photon absorption process. Indeed, from Eq. (1) and Eq. (4), one gets

$$\frac{H}{M(T)}=\frac{H_{\mathrm{zero}}}{M(T+\Delta T)} \tag{5}$$

and ΔT is extracted from this implicit equation. The determination of the cluster specific heat at a given initial temperature T is then straightforward: $C(T) = \hbar\omega / \Delta T$.

The procedure presented here for the absolute determination of the cluster specific heat is very demanding and becomes intractable at high temperature ($T > 500$ K) where deflections are small. Consequently the absolute measurement of the specific heat is performed solely at room temperature. An alternative method, described below, is then used to determine higher temperature values of the specific heat. When applied similarly at room and higher temperatures, it leads to the determination of the specific heat at high T relatively to its absolute value at room temperature.

C. Relative determination of the cluster specific heat

The method used for the relative measurement of the specific heat consists of two distinct steps which use similar concepts. In the first step, measurements are done at room temperature. The cluster beam is heated with the laser, using several different light intensities and the ratio $(\langle d(I)\rangle - d_0)/\langle d(I)\rangle$ is plotted as a function of the light intensity I. Here, d_0 is the cluster beam deflection at a given field without heating, and $\langle d(I)\rangle$ the deflection of the cluster beam heated with a light intensity I, at the same previous field value. Both d_0 and $\langle d(I)\rangle$ are extracted from their respective experimental profiles, as described in the experimental section. From Eq. (1) and Eq. (2), the deflection ratio is

$$\frac{(\langle d(I)\rangle - d_0)}{\langle d(I)\rangle} = 1 - \frac{M(T)}{\sum_{n\geqslant 0} M(T+n\Delta T)P(n,\beta I)}. \qquad (6)$$

The magnetization curve $M(T)$ is known from previous measurements while ΔT could be extracted from the room temperature value of the specific heat obtained by the above calibration. Thus, the photoabsorption cross section β, appearing in the Poisson distribution, is the only free parameter in Eq. (6). It can be obtained by a fit to the experimental deflection ratio values. The summation in Eq. (6) is truncated to obtain the optimal β value (typically $n_{max} = 10$).

Knowing β, we can deduce the mean number of interacting photons for a given light intensity, $\langle n\rangle = \beta I$. We found that, for $Fe_{120-140}$ in Fig. 3 and Fig. 4, $I \approx 40$ corresponds to $\langle n\rangle \approx 1$. At $I = 15$, a typical intensity for the absolute determination of the specific heats (see Fig. 3), the probability to absorb (0,1,2,3, . . .) photons is (0.69, 0.25, 0.05, 0.006, . . .) respectively and thus can be considered as a low intensity limit. Similarly, for the relative measurements at $I = 80$ in Fig. 4, the probability to absorb more than 6 photons becomes negligible ($\approx 1.2\%$).

Figure 4 shows typical deflection ratios and fits for iron and cobalt clusters. The dependence of the ratio $(\langle d(I)\rangle - d_0)/\langle d(I)\rangle$ on the intensity is linear in the case of cobalt clusters and highly nonlinear for iron clusters. In this last case, the deviation from the linear behavior is due to the peculiar dependence of the iron magnetic moment on temperature. Once β is known for a given cluster type, it is not necessary to measure it again, except when the light path of the heating laser is altered. This is because the value of I that we measure in our experiment is only proportional to the fluence of the heating laser light in the interaction region. The proportionality constant varies with the exact position of the beam with respect to the magnet poles and the heating laser power meter.

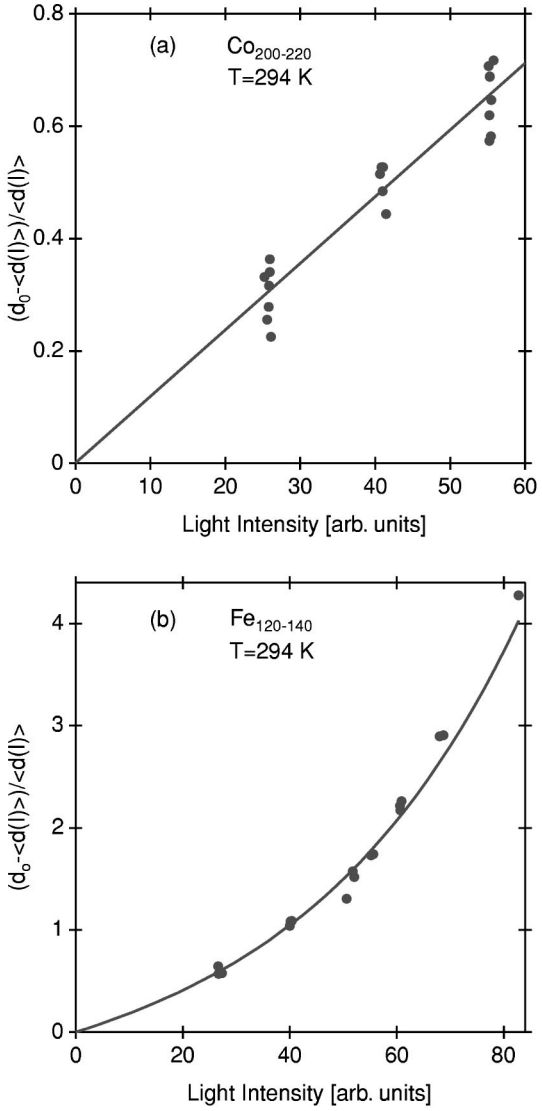

FIG. 4. The determination of the photoabsorption cross section of $Co_{200-240}$ and $Fe_{120-140}$. The measured points correspond to the normalized difference in deflection between beam of clusters that have not been heated (deflected by an amount d_0) and the beam of clusters that have been heated with a laser of intensity I [deflected by an amount $\langle d(I)\rangle$]. The experimental data is well fitted by the model of absorption we have assumed (continuous curve). The only free parameter of the curve is the value of β, the photoabsorption cross section. In $Co_{200-240}$ (a) the curve is a straight line since the magnetic moment per atom is fairly constant up to 900 K. In $Fe_{120-140}$ (b) the magnetic moment per atom falls quickly near 350 K and is responsible for the nonlinear curve.

In the second step, identical measurements are done, but at higher temperatures. Again, the experimental deflection ratio, $(\langle d(I)\rangle - d_0)/\langle d(I)\rangle$, is plotted against I. Since we assumed that β does not depend on cluster temperature, the only free parameter left is ΔT. Thus, the fit to experimental values gives the cluster temperature increase due to the one-photon absorption process. As a result, the specific heat value as a function of the temperature can be deduced.

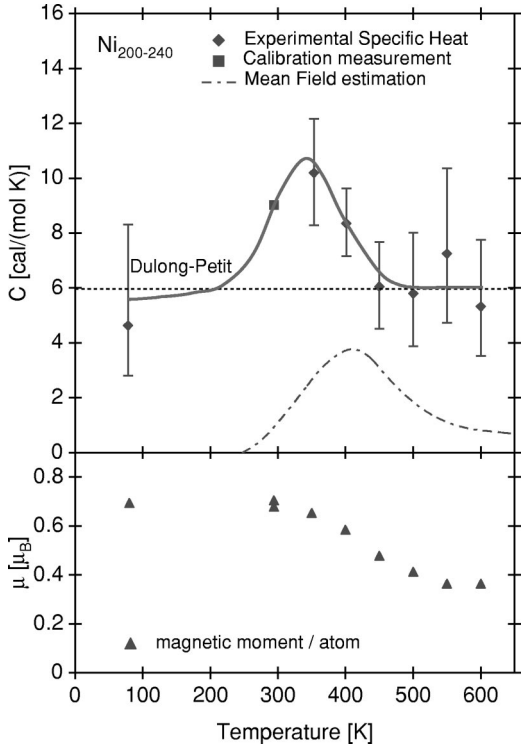

FIG. 5. Specific heat of $Ni_{200-240}$ clusters. The experimental specific heat is displayed using black diamonds in the upper part of the graph. The calibration (absolute) measurement has been done at room temperature and is displayed as a black square. The other measurements are relative ones. The error on the calibration is $\pm 17\%$ and arises mainly from the determination of H_{zero}. The horizontal dashed line is the Dulong-Petit value of the specific heat. The dash-dot curve is the magnetic contribution to the specific heat in the mean field approximation. Finally, the continuous curve is a guide to the eyes. The experimental magnetic moment per atom is displayed using black triangles in the lower part of the graph. The unit is the Bohr magneton ($\mu_B = 9.2741 \times 10^{-24}\ J/T$).

IV. RESULTS AND ANALYSIS

The results of the specific heat measurements are presented in Figs. 5 and 6 together with the corresponding curves of the magnetic moment per atom as a function of temperature. The specific heat of a small ferromagnetic cluster system is expected to be composed of different contributions. The main contribution to the specific heat comes from the lattice vibrations. If we consider only the harmonic terms in the ionic interaction potential, it should converge to the classical Dulong-Petit value [6 cal/(mol K)] at temperatures higher than the Debye temperature.[20] The cluster Debye temperature is expected to be reduced compared to its bulk counterpart since long wavelength excitations cannot be sustained in a finite system.[8] Furthermore, apart from the electronic specific heat due to the valence electrons, the other contributions are related to one or more possible phase transitions that could occur in the cluster. For instance, it could undergo a structural phase transition, from one structure to another one, or it could melt. In the case of a magnetic system, we also expect to see a contribution from the magnetic phase transition prominent near the Curie point.

Summarizing, we write for the total specific heat[27]

$$C(T) = C_{lat}(T) + C_{el}(T) + C_{trans}(T), \tag{7}$$

where $C_{lat}(T)$ is the lattice and $C_{el}(T)$ the electronic specific heats and $C_{trans}(T)$ represents contributions to the specific heat from the different phase transitions.

For ferromagnetic bulk iron, cobalt and nickel, the specific heat around the Curie temperature and the magnetic moment are intimately related. The magnetic moment is deduced from the saturation magnetization. The ferromagnetic to paramagnetic transition is a second order phase transition which manifests itself by the loss of long-range ferromagnetic order. At the Curie temperature, the magnetic moment value converges to zero and correspondingly the specific heat reaches its maximum value. Despite some limitations (see, for instance, Refs. 19 and 20), the mean field, or Weiss, model allows a reasonable approximation of the magnetic contribution to the total specific heat. In the framework of this model, the specific heat is given by[19]

$$C_M(T) = -\frac{3Nk_BT_C}{2\mu_0^2}\,\frac{j}{j+1}\,\frac{d\mu_{at}^2(T)}{dT}, \tag{8}$$

where N is the number of atoms, T_C is the Curie temperature, μ_0 is the magnetic moment per atom, $j = \mu_0\mu_B^{-1}g^{-1}$ (g is the gyromagnetic ratio), and $\mu_{at}(T)$ is the temperature dependent magnetic moment.

In bulk ferromagnetic transition metals, this approximation reproduces relatively well the shape and area of the specific heat associated with the magnetic phase transition. This is true provided the experimental value of T_C is used since the mean field model does not give a good quantitative estimate of it. We have used a similar approach for the ferromagnetic clusters. The mean field specific heat is deduced from Eq. (8) using the experimental curve of the magnetic moment per atom versus temperature, $\mu(T)/N$. This computed contribution to the specific heat, which has a purely magnetic character, is then compared to the measured specific heat curve.

A. Nickel and cobalt clusters

The measurements on $Ni_{200-240}$ clusters (Fig. 5) lead to a specific heat curve $C(T)$ which is easily interpreted in this general frame. There is a broad peak centered at $T = 340$ K which adds to an approximately constant value of 6 cal/(mol K) over the whole measurement range, 90–600 K. The position and the area of this peak are reasonably well approximated by the mean field model estimate of the specific heat. Therefore, this peak certainly has a magnetic origin and the associated transition is the equivalent of the Curie point in bulk nickel. The maximum of the mean field curve, which defines the Curie temperature in this case,[21] is at $T = 420$ K, which is lower than its bulk counterpart, 625 K. Note that the maximum of $C(T)$ occurs at a lower temperature than that derived from the mean field approximation. The reason for this shift may be the mean field model overestimation of the transition temperature because it neglects the fluctuations.[28] Integration of the specific heat peak shows that the heat associated with the transition is 530 cal/mol (0.022 eV/atom) which is higher than its bulk counterpart, 420 cal/mol (0.018 eV/atom).[27] The origin of this difference could be the en-

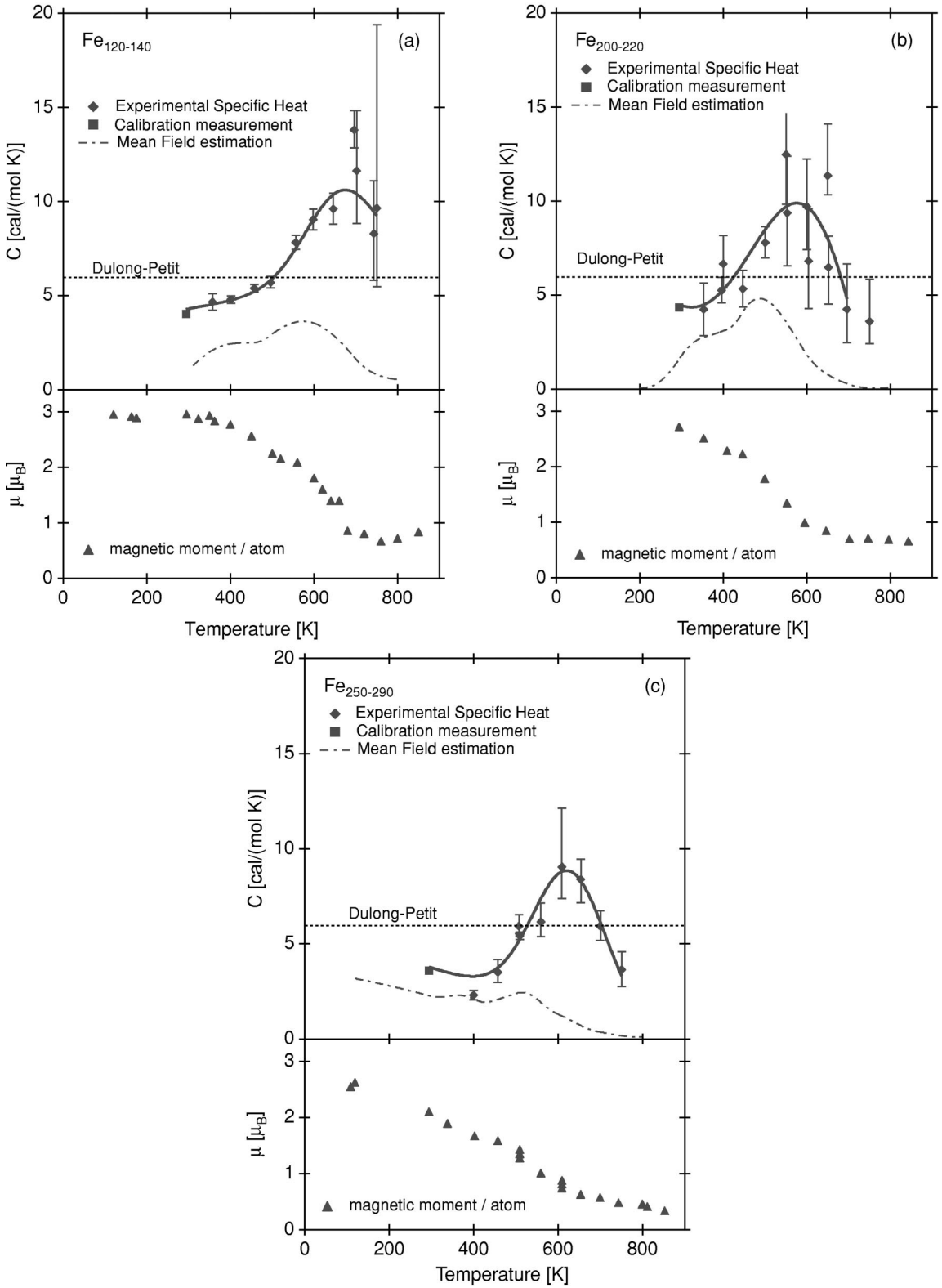

FIG. 6. Specific heat of iron clusters of increasing size range [(a) 120–140 atoms, (b) 200–220 atoms, and (c) 250–270 atoms]. The symbols are the same as the ones used in Fig. 5. The error on the calibration is (a) $\pm 11\%$, (b) $\pm 32\%$, and (c) $\pm 20\%$. The most striking feature of the specific heat is its low value around room temperature, for all size ranges. Notice how, in the case of 200–220 and 250–290 atoms clusters, the specific heat stays low when the magnetic moment starts to decrease in the 200–400 K temperature range.

hanced magnetic moment of clusters compared to the bulk, but the experimental error bars and the somewhat arbitrarily selected baseline in the integration of the peak make any conclusion difficult.

There are no prominent features in the experimental specific heat curve of $Co_{200-240}$ clusters. We observe a steady increase from 5.5 cal/(mol K) at 300 K to 15 cal/(mol K) at 900 K. Unfortunately, measurements at higher temperatures

to check the evolution of the specific heat curve cannot be achieved with our experimental setup. Further details and discussions are reported in Refs. 16 and 17.

B. Iron clusters

First, we present the specific heat of iron clusters in several different size ranges, 120–140 atoms, 200–220 atoms, and 250–290 atoms. The results (Fig. 6) are at first sight similar to the specific heat curve of $Ni_{200-240}$ clusters, showing a wide and distinct specific heat peak. However, combining a harmonic lattice specific heat with a contribution from a ferromagnetic to paramagnetic transition does not model accurately the experimental data.

First, the specific heat of iron clusters in the temperature range 300–400 K is anomalously low, going down to 3 cal/(mol K) in the case of $Fe_{250-290}$. This is significantly lower than the Dulong-Petit value. If the only contribution to the specific heat was the harmonic lattice contribution, then the Debye temperature of $Fe_{250-290}$ clusters, obtained by fitting a Debye specific heat curve to the lowest value of the measured specific heat, would be approximately 2000 K. Comparing this to the bulk value, $\theta_D = 425\ K$,[20] shows that the Debye model is not suited to describe iron clusters.

Secondly, the mean field model does not correctly reproduce the wide specific heat peak that we observe. This is apparent in the case of the $Fe_{250-290}$ clusters where the mean field model predicts a contribution of the magnetic system to the specific heat which is roughly constant up to 550 K where it decreases, whereas the measured specific heat shows a very distinct peak around 600 K. Moreover, contrarily to the Ni case where the mean field analysis overestimates the position of the specific heat maximum as it could be expected,[28] in the case of iron clusters the mean field underestimates it.

Third, there is a temperature shift between the magnetic moment decrease and the specific heat peak for each cluster size.

Fourthly, the experimental values do not converge to the bulk specific heat curve when the cluster size is increased. For the largest size range that we measured (370–420 atoms, not presented) the specific heat at 377 K is still as low as $3.84 + 0.17 - 0.3$ cal/(mol K). The specific heat peak, which is observed at $T = 650$ K in $Fe_{120-140}$ clusters, stays around $T = 600$ K in $Fe_{200-220}$ and $Fe_{250-290}$ clusters. This shows no sign of convergence towards the bulk iron value although we would expect this peak to shift to higher temperatures with increasing sizes.

The anomalies, namely the low specific heat and the failure of the mean field model, get more pronounced when the size is increased from 130 to 270 atoms, and more generally, there is no sign of convergence towards the bulk behavior upon increasing the size. These observations suggest that iron clusters, unlike nickel ones, do not undergo a simple ferromagnetic to paramagnetic transition. This leads us to question the mechanism that drives the magnetic transition in Fe clusters. We consider four possible hypothesis: the presence of metastable isomers in the beam, the melting of the clusters, a surface demagnetization and finally a high moment–low moment (HM-LM) magnetic transition.

a. Metastable clusters? It is tempting to consider the presence of metastable isomers in the beam to explain the low specific heat. The presence of isomers in iron clusters produced by laser vaporization has been invoked to explain why the determination of the iron cluster structure in a molecular beam experiment is a difficult task.[29] In this hypothesis, some energy is released when the clusters go from the metastable state to a lower energy state after the interaction with photons. This makes the estimation of the specific heat difficult because one does not know the total energy that contributes to the cluster heating. Indeed, if one considers only the impinging photon energy, this underestimation leads to an incorrect, low value of the specific heat. When a Fe_{270} cluster at 300 K interacts with a single 532 nm photon, its temperature goes up by approximately 68 K. Using a simple Arrhenius law to model the decay of the cluster metastable state leads to the following conclusion. If such a low temperature increase is enough to anneal the clusters and cause a relatively large error in the determination of the specific heat, then a large proportion of the clusters should anneal spontaneously in flight even in the absence of heating, and the cluster mean temperature should increase markedly during the time they spend in the beam before entering the magnet (≈ 1 ms). Slow clusters should then be hotter (hence their magnetization should be lower) than fast clusters, because they have more time to anneal before interacting with the magnetic field, but we did not observe such a behavior. Although we do not know anything about the presence of isomers in the beam we can exclude their presence as a cause for the low specific heat.

b. Melting? Cluster melting can induce a specific heat increase in the critical region,[13] equivalent to the latent heat of fusion in the bulk, as well as a partial or total loss of magnetic order which is a consequence of the structural change. While the wide specific heat bump in iron clusters of various sizes is not well described in the frame of the mean field model, the area under the peak (approximately 1300 cal/mol in the case of $Fe_{120-140}$, $Fe_{200-220}$ and $Fe_{250-290}$ clusters) is lower than the total energy of the ordered spin system, which is itself, in bulk iron, about 60% of the latent heat of fusion. If the iron clusters did really undergo a melting transition around 600 K, then the associated specific heat increase would reflect the melting as well as the ferromagnetic transition. This would lead to values of the specific heat higher than the ones we measured. This model has another flaw. The magnetic moment per atom of $Fe_{250-290}$ decreases in a temperature range where no increase in specific heat is observed. Indeed, at 350 K, the specific heat is anomalously low whereas the magnetic moment decrease is already visible. This is incompatible with a model where the melting drives the magnetic transition. These observations lead to the conclusion that there is probably no melting occurring in iron clusters, in the size and temperature ranges we considered.

c. Surface demagnetization? The Curie temperature of surfaces is known to be lower than the bulk one,[30] mainly as a result of the lower coordination. But the gradual, almost linear decrease in magnetic moment that we observe in $Fe_{250-290}$ clusters cannot be described by a model where the iron cluster surface, or the outermost shell, has a lower Curie temperature than the inner shells. If it were the case, then the smaller $Fe_{120-140}$ clusters would show an even more rapid decrease of their magnetic moment than the larger clusters

do, since they have proportionally more atoms on the surface. Our measurements on iron clusters do not show this kind of behavior.

d. HM-LM transition? Finally, let us consider the possibility of a magnetic transition by first reviewing some peculiarities of the coupling between structure and magnetism in iron. Under normal conditions, the crystalline structure of bulk iron changes from bcc to fcc at 1185 K, i.e., 142 K above the Curie temperature. The bcc structure disappears when the short-range ferromagnetic order vanishes. When the exchange interaction term in the Hamiltonian of iron is not taken into account, the computed bulk iron structure is fcc, instead of bcc when the full Hamiltonian is used.[31] Consequently the iron structure is related to its magnetic coupling and a modification of its structure may induce a magnetic property change. Such an extreme sensibility of the magnetic properties on the geometrical environment is neither observed nor predicted for Ni and Co.[32–34]

The iron fcc structure is stable only between 1185 K and 1663 K. The magnetic and structural properties of fcc iron at temperatures lower than 1185 K are scarcely known. It has been theoretically predicted[35,36] that fcc iron could exist in at least two different magnetic states: a high moment, high volume state [$\mu=(2.3–2.8)\ \mu_B$/atom, lattice constant $\geqslant 3.6$ Å] and a low moment one ($\mu \leqslant 1.6\ \mu_B$/atom, with a lattice constant between 3.5 and 3.6 Å). Fcc iron is also believed to exhibit strong magnetovolume effects and a noncollinear magnetic structure under compression.[35,37] The experimental situation is confusing. An antiferromagnetic low moment ($\approx 0.7\ \mu_B$ /atom) state, denoted γ_1, with a Neel temperature of about 67 K has been identified, for instance in fcc iron precipitates in supersaturated Fe-Cu alloys.[38] On the other hand, ferromagnetic fcc stable states, usually denoted γ_2, have been reportedly observed in certain Fe solid solutions which adopt the fcc structure or from thin iron films grown on a fcc substrate.[39] In the latter case, external constraints are applied to force the samples to adopt the fcc geometry.

Different stable geometric structures, which are impossible or thermodynamically unstable in the bulk, are currently observed in nanometer size materials.[40] In the case of iron clusters, we have clues about the structural parameters through indirect measurements. For instance, EXAFS measurements on iron particles with diameters down to 9 Å embedded in solid argon at 4.2 K indicate that their structure is close to the bcc bulk one.[41] Smaller iron clusters have a structure consistent with a hcp or fcc bulk environment. More relevant to our work is a recent magnetic property study on pure ball-milled Fe crystallites with diameter around 10 nm.[42] These supported nanocrystals can be heated up to 700 K readily. Mössbauer spectroscopy and HRTEM are consistent with a bcc structure of the crystallites. However, annealing the particles to 570 K for 1 h transforms the structure at the grain boundaries to fcc. This new iron phase shows a reversible order-disorder magnetic transition at approximately 500 K. It has been interpreted as a ferromagnetically ordered γ_2-Fe phase having a lower magnetic moment compared to the bcc phase.

The structures or the most common isomers of free iron clusters in the size range 100–1000 atoms are not yet known. Near threshold photoionization and time of flight mass spectroscopy[29] at room temperature do not allow the assignment of a single structure to iron clusters. Nevertheless, it has been suggested that iron clusters probably do not keep the same structure over a large temperature range. Indeed, clusters having less than 200 atoms show a different structured mass spectrum than larger clusters, probably indicating a structural change. Therefore, the exact structure of free iron clusters is unknown, and could even change with temperature. On the other hand, theoretical studies on complex systems like iron aggregates with as much as 1000 atoms are notoriously difficult. Using an empirical many-body potential, it has been shown[43] that various cluster structures with different symmetries have a similar energy in the 100–1000 atoms size range, actually leaving the question open.

By analogy with the results of Del Bianco *et al.*,[42] we believe that a HM-LM transition could play an important role in free iron clusters containing a few hundred of atoms. In this sense, iron clusters would behave like the γ_2-Fe phase at the grain boundaries of a nanocrystalline powder. A high moment state is energetically favored at low temperatures, but a low moment magnetically ordered state exists at a higher energy, and can be thermally excited as it has been proposed for Invar systems.[44] The gradual transition from the HM state to the LM state with increasing temperature produces the observed decrease in the magnetic moment, but no augmentation of the specific heat. Indeed, a magnetic order exists for both HM and LM configurations and therefore the entropy increase is only minimal. Since the LM state reaches its Curie temperature well before the HM state, it loses its order at moderate temperatures (500–600 K), raising the entropy of the magnetic system. This transition causes a specific heat increase but only a modest change in the magnetic moment. This model describes qualitatively our magnetic moment measurements and could explain the mean field model failure as well as the temperature shift between the magnetic moment decrease and specific heat peak. However, it does not describe the low specific heat at room temperature and does not address why, upon increasing the size, the iron cluster specific heat deviates more strongly from the bulk behavior.

These particular features could result from the shape of the interatomic potential which is a consequence of the existence of two distinct magnetic states with different lattice parameters.[42] Suppose that the ionic interatomic potential has a double well shape.[35] One well corresponds to the HM state and the other one, at a higher energy and with a lower lattice constant, arises from the metastable LM state. Unlike a purely harmonic interaction, this peculiar interatomic potential has not equidistant energy levels. In an energy range close to the metastable state energy, the distribution of the vibrational levels is modified.[45] For instance, the energy gap between two consecutive levels could be increased compared to the harmonic case and thereby affects the thermal behavior of the system. The vibrational specific heat could exhibit a two-bump structure, in which case the classical Dulong-Petit value is reached well above the Debye temperature. Thus, unlike a purely harmonic interatomic potential, a two-state model with a double well shape ionic interaction potential may explain the low value of the room temperature specific heat.

Moreover, in such a double well potential, the transition between the HM to the LM states is governed by many fac-

tors: the energy difference and the energy barrier between the HM and the LM states, and the exact details of the potential wells. Since the size of the iron clusters is very small, we believe that these parameters might fluctuate from size to size. For instance, $Fe_{250-290}$ could possibly have a lower energy barrier than $Fe_{120-140}$, and therefore it would transform at a lower temperature and over a broader temperature range. Since we do not know the exact interatomic potential landscape, this last suggestion deserves further attention.

V. CONCLUSION

We have presented a detailed method for the measurement of the specific heat of free ferromagnetic clusters. The only requirement for this type of measurement is the existence of a physical property of the clusters which varies monotonically with temperature and can be measured in flight. While the specific heat of nickel clusters, and to a lesser extent cobalt clusters, is consistent with simple theoretical predictions based on the mean field model of ferromagnetism, iron clusters show an anomalous thermal behavior. The specific heat is low particularly around 300–400 K, and its peak cannot be explained invoking a mean field argument. Although we suggested a mechanism to account for these experimental observations, the magnetism of iron remains a complicated topic that has not delivered all its secrets.

ACKNOWLEDGMENTS

We are indebted to the Swiss National Science Foundation for financial support. We would like to thank J.-M. Bonard, N. Desmarais, and S. Fakra for valuable discussions and comments.

*Email: gerion@uclink4.berkeley.edu Present address: Department of Chemistry, University of California, Berkeley, CA 94720.

†Permanent address: Institut de Génétique et Biologie Moléculaire et Cellulaire, Laboratoire de Biologie Structurale, 67404, Illkirch, France.

‡Permanent address: School of Physics, Georgia Institute of Technology, Atlanta, GA 30332-0430.

[1] Y. Imry, Phys. Rev. B **21**, 2042 (1980).

[2] X. Yu and P. M. Duxbury, Phys. Rev. B **52**, 2102 (1995); R. Poteau, F. Spiegelmann, and P. Labastie, Z. Phys. D: At., Mol. Clusters **30**, 57 (1994); N. Ju and A. Bulgac, Phys. Rev. B **48**, 2721 (1993); D. Reichardt, V. Bonacic-Koutecky, P. Fantucci, and J. Jellineck, Z. Phys. D: At., Mol. Clusters **40**, 486 (1997).

[3] P. Pawlow, Z. Phys. Chem., Stoechiom. Verwandtschaftsl. **65**, 1 (1909); **65**, 545 (1909).

[4] R. S. Berry, J. Jellineck, and G. Natanson, Phys. Rev. A **30**, 919 (1984).

[5] P. Labastie and R. L. Whetten, Phys. Rev. Lett. **65**, 1567 (1990).

[6] V. Wildpaner, Z. Phys. **270**, 215 (1974).

[7] P. V. Hendriksen, S. Linderoth, and P.-A. Lindgård, Phys. Rev. B **48**, 7259 (1993); P. V. Hendriksen, S. Linderoth, and P.-A. Lindgård, J. Magn. Magn. Mater. **104**, 1577 (1992).

[8] A. Tamura, K. Higeta, and T. Ichinokawa, J. Phys. C **15**, 4975 (1982); **16**, 1585 (1983).

[9] Y. Volokitin, J. Sinzig, G. Schmid, H. Bönnemann, and L. J. De Jongh, Z. Phys. D: At., Mol. Clusters **40**, 136 (1997); Y. Volokitin, J. Sinzig, L. J. de Jongh, G. Schmid, M. N. Vargaftik, and I. I. Moiseev, Nature (London) **384**, 621 (1996).

[10] V. Novotny and P. P. M. Meincke, Phys. Rev. B **8**, 4186 (1973).

[11] C. C. Chen, A. B. Herhold, C. S. Johnson, and A. P. Alivisatos, Science **276**, 398 (1997).

[12] S. L. Lai, J. Y. Guo, V. Petrova, G. Ramanath, and L. H. Allen, Phys. Rev. Lett. **77**, 99 (1995).

[13] M. Schmidt, R. Kusche, B. von Issendorf, and H. Haberland, Nature (London) **393**, 238 (1998); M. Schmidt, R. Kusche, W. Kronmüller, B. von Issendorf, and H. Haberland, Phys. Rev. Lett. **79**, 99 (1997).

[14] Ph. Buffat and J.-P. Borel, Phys. Rev. A **13**, 2287 (1976); A. N. Goldstein, C. M. Echer, and A. P. Alivisatos, Science **256**, 1425 (1992).

[15] I. M. L. Billas, A. Châtelain, and W. A. de Heer, Science **265**, 1682 (1994).

[16] I. M. L. Billas, A. Châtelain, and W. A. de Heer, J. Magn. Magn. Mater. **168**, 64 (1997).

[17] A. Hirt, D. Gerion, I. M. L. Billas, A. Châtelain, and W. A. de Heer, Z. Phys. D: At., Mol. Clusters **40**, 160 (1997).

[18] J. A. Becker and W. A. de Heer, Ber. Bunsenges. Phys. Chem. **96**, 1237 (1992).

[19] E. C. Stoner, *Magnetism of Matter* (Methuer and Co. Ltd., London, 1934).

[20] N. W. Ashcroft and N. D. Mermin, *Solid State Physics* (Holt, Reinhart, Winston, New York, 1976).

[21] *Cindas Data Series on Material Properties*, edited by Y. S. Touloukian and C. Y. Ho (McGraw-Hill, New York, 1981), Vol. III-1.

[22] W. A. de Heer and P. Milani, Rev. Sci. Instrum. **61**, 1835 (1990); **62**, 670 (1991).

[23] E. Beaurepaire, J.-C. Mercel, A. Daunois, and J.-Y. Bigot, Phys. Rev. Lett. **76**, 4250 (1996).

[24] C. P. Bean and J. D. Livingston, J. Appl. Phys. **30**, 120s (1959); S. N. Khanna and S. Linderoth, Phys. Rev. Lett. **67**, 742 (1991).

[25] Once the specific heat curve is known from the method described in Secs. III B and III C, an iterative calculation can be made to take into account the difference between $\Delta T_1, \Delta T_2, \ldots, \Delta T_n$. In this case, the specific heat is $C = \Delta E / \Delta T_1$ by definition. This is accomplished in this way. For a given temperature, we estimate $\Delta T_1, \Delta T_2, \ldots, \Delta T_n$. We fit the experimental data of Fig. 4 using the generalized formula $\langle M \rangle = \Sigma_{n \geq 0} M(T + \Delta T_n) P(n, \beta I)$ instead of Eq. (2). ΔT_1 is optimized while $\Delta T_2, \ldots, \Delta T_n$ are kept constant. This seems reasonable since ΔT_1 is the parameter that affects mainly the fit. This iterative calculation does not lead to any significant modification in the shape and peak position of the specific heat curves. The peak areas are subjected to a modest change ($\approx 5\%$) that is not significant considering the large error bars.

[26] This analysis method considers only a particular point of the profile shape (named r^* in the text) but the requirement must be the equivalence of the profile shapes $\psi_1(r, H)$ and $\psi'(r, H')$ for each position r. We checked the reliability of our method by simulating deflection profiles that have a width proportional to their deflection as the experimental ones have. Then we summed up two or three of them to get a test profile and simulate Eq. (3). Some noise was added to the test profile. By knowing one of its components, our method was able to find the other ones. A

detailed discussion can be found in D. Gerion, diploma work, EPF Lausanne, 1995.
[27] J. A. Hofmann, A. Paskin, K. J. Tauer, and R. J. Weiss, J. Phys. Chem. Solids **1**, 45 (1956).
[28] D. Chandler, *Introduction to Modern Statistical Mechanics* (Oxford University Press, New York, 1987).
[29] M. Pellarin, B. Baguenard, J. L. Vialle, J. Lermé, M. Broyer, J. Miller, and A. Perez, Chem. Phys. Lett. **217**, 349 (1994).
[30] M. Przybylski, J. Korecki, and U. Gradmann, Appl. Phys. A: Solids Surf. **52**, 33 (1991).
[31] D. G. Pettifor, J. Phys. C **3**, 1967 (1970); G. Grimvall, Phys. Scr. **13**, 59 (1976).
[32] I. Turek and J. Hafner, Phys. Rev. B **46**, 247 (1992).
[33] R. F. Sabiryanov, S. K. Bose, and O. N. Mryasov, Phys. Rev. B **51**, 8958 (1995).
[34] M. Liebs, K. Hummler, and M. Fahnle, Phys. Rev. B **51**, 8664 (1995).
[35] V. L. Moruzzi, Solid State Commun. **83**, 739 (1992).
[36] O. N. Mryasov, A. I. Liechtenstein, L. M. Sandratskii, and V. A. Gubanov, J. Phys.: Condens. Matter **3**, 7638 (1991).
[37] R. F. Sabiryanov and S. S. Jaswal, Phys. Rev. Lett. **83**, 2062 (1999).
[38] S. C. Abrahams, L. Guttmam, and J. S. Kasper, Phys. Rev. **127**, 2052 (1962); T. Majima, T. Miyahara, K. Haneda, and M. Takami, Jpn. J. Appl. Phys., Part 2 **33**, L223 (1994); N. Heiman and N. Kazama, Phys. Rev. B **19**, 1623 (1979).
[39] P. A. Montano, G. W. Fernando, B. R. Cooper, E. R. Moog, H. M. Naik, S. D. Bader, Y. C. Lee, Y. N. Darici, H. Min, and J. Marcano, Phys. Rev. Lett. **59**, 1041 (1987); P. Crespo *et al.*, Phys. Rev. B **48**, 7134 (1993).
[40] A. P. Alivisatos, Science **271**, 933 (1996).
[41] P. A. Montano, J. Zhao, M. Ramanathan, G. K. Shenoy, and W. Schulze, Z. Phys. D: At., Mol. Clusters **12**, 103 (1989).
[42] L. Del Bianco, C. Ballesteros, J. M. Rojo, and A. Hernando, Phys. Rev. Lett. **81**, 4500 (1998).
[43] N. A. Besley, R. L. Johnston, A. J. Stace, and J. Uppenbrink, J. Mol. Struct.: THEOCHEM **341**, 75 (1995).
[44] M. van Schilfgaarde, I. A. Abrikosov, and B. Johanson, Nature (London) **400**, 46 (1999).
[45] D. Gerion, Ph.D. thesis, EPF Lausanne, 1999.